Test Methodology for the Investigation of Environmental Effects on Corrosion Fatigue

Justin Rausch,,*** Sarah Galyon Dorman*, and Dr. Scott Fawaz**

SAFE, Inc.

ARTICLE INFO

Article history:

Received Day Month Year
Accepted Day Month Year
Available Day Month Year

Keywords:

Corrosion Fatigue
Aluminum
Atmospheric Environments
Test Methodology

*SAFE Inc., 3290 Hamel Cir, Monument, Colorado 80132

***Corresponding author: +1719.375.5855
Email: jwr@saf-engineering.com.

ABSTRACT

The objective of this work was to develop a test methodology for corrosion fatigue that allows researchers to investigate the effects of environmental parameters on fatigue crack growth rates of cracks nucleating from corrosion pits. Environmental factors are important as small changes in crack growth rates while the crack is small can have large effects on the overall life of structural components due to the exponential nature of fatigue crack growth. The effect of changing environments on the crack growth rate is important to the corrosion fatigue community as chromate containing primers and protective coatings are thought to help protect components during this mechanically small crack growth regime by chemically altering the local environment around the crack tip. The chromate protection offered in the early stages of crack growth can become very significant to structural part life as the effect of chromate is potentially lessened as the crack becomes larger. This is due to the environment having less of an influence on crack growth as the mechanical crack driving force overcomes the environmental effect as crack length increases. The current push for reduction in chromate containing coatings due to health and environmental concerns could have an unintended consequence that component lives will suffer due to the removal of the chromate corrosion protection. The test methodology developed herein, was designed to address the potential reduction in life by providing a test platform where the effects of varying environmental factors on the crack growth of small cracks could be fully investigated.

INTRODUCTION

Corrosion pits in aircraft structure have long been known for their role in crack nucleation [1]. The significance of corrosion pits in aircraft structure with respect to aircraft maintenance can be differentiated by the maintenance philosophy of the aircraft. The two primary methods for maintaining the structural integrity of military aircraft currently in use today, damage tolerance and safe life, tend to ignore these small cracks nucleating from pits. For a given crack that nucleates from a corrosion pit, the majority of the component life is spent nucleating and growing the crack below the initial flaw sizes considered in both damage tolerant and safe-life design. These small cracks from pits are therefore of no consequence to fleet managers using damage tolerant designs because such small crack growth occurs in the time to propagate the 1.27 mm rogue flaw, already assumed to be present in the component. The safe-life management approach uses some of this initial flaw information to make assumptions when calculating component life, but does not allow for extension of component life beyond its designed life. While the two design methodologies do not account for the cracks below the initial assumed flaw sizes, environment and the coatings protection of the component can have great influence on the rate at which these small cracks propagate. The additional data generated by this test method could provide valuable information, that when used in conjunction with predictions based on usage and environment, allow maintainers to equate damage accumulation during component life to make fracture mechanics based predictions beyond the components original designed life. Furthermore, any change in the part coating or environment that may be more aggressive or beneficial may not be accounted for in the component life. To be conservative, safe-life methodology uses a harsher environment to calculate the time required to propagate a crack to 0.25 mm. Research into chromate coatings [2] have shown a reduction in crack growth rates in the long crack lengths, however influences in the crack growth rates in the small crack range can be even more significant. The exponential nature of crack growth can magnify any small change in either crack nucleation time, or crack growth rate, resulting in large changes to the total life of the component. Currently it is not fully understood what level of protection chromate provides during early crack growth, nor is there a standardized test methodology for research to produce quality, comparable data. The push for less toxic materials is changing the chemistry of primers and corrosion preventative coatings used on aircraft and full consequences of the changes should be understood by designers and maintainers prior to implementation. This test protocol was designed to give researchers a tool which can provide data to evaluate these small changes in crack growth allowing better prediction and modeling techniques for cracks nucleating from corrosion pits.

Experimental Procedures

A standard specimen was designed and used throughout this test method. The specimen gage section featured an open hole 6 mm in diameter, with a rectangular cross-section 10 mm wide and 3.2 mm thick. For ease of manufacture the specimen had 11.11 mm diameter cylindrical ends with 6.35 mm radii on the transition between the cylindrical ends and the rectangular gage section. The specimen was designed such that its geometry would be representative of aircraft skin and fastener configurations commonly found in aircraft structural design. Figure 1 shows an overview of the open hole specimen, as well as provides typical geometric dimensions. For this test program the open hole specimen was fabricated from 50.8 mm thick aluminum alloy 7075-T651 plate. During fabrication the specimen orientation was

kept aligned such that fatigue tests would be performed with the crack growing in the L-T direction. During specimen fabrication care was taken to locate the specimen centerline at a distance of 8.47 mm from the top and bottom surface of the plate. Specifying the thickness location from the surface of the aluminum plate was done to minimize any through-thickness variations that may affect the mechanical properties of the specimens. The material selection for this test program was aluminum plate originally produced for the Defense Advanced Research Projects Agency (DARPA) Structural Integrity Prognosis System (SIPS) program. The material used in the SIPS program was produced in a manner which replicated legacy aluminum alloys by keeping historically relevant material compositions [3] including typical amounts of contaminates relevant to the legacy material production. The most attractive feature of the SIPS material was the degree of material characterization performed, particularly the quality of the fatigue crack growth rate curves. The material characterization, particularly that of the fatigue performance, allowed for comparisons to be made between the open hole data generated from this work, and the previously generated characterization data. All data generated and compared herein was procured from the same lot of material to eliminate lot-to-lot material variances.

Since this method was focused on the change in fatigue crack growth rate under various environments, an automated method of fatigue crack length (and by extension rate) monitoring was needed. Based on the needed accuracy, automation, and durability, Direct Current Potential Drop (DCPD) [4] was used. Fundamentally DCPD works by passing a constant current though a material and measuring the change in voltage as a crack grows through the material. Two probes are spot welded to the specimen surface and because there is a fixed amount of material between the two probes there is also an associated fixed resistance between the two DCPD leads. Once a fatigue crack forms, there is less continuous material between the two leads and as a result less resistance. Based on Ohm's law, as the resistance decreases so does the voltage given that the current remains constant. Using this method of crack detection provides multiple advantages. DCPD probes can be placed in positions not possible or practical with conventional measurement techniques, DCPD is automated, and the required size of the DCPD probes are small. As only a small amount of the probe needs to be in contact with the specimen surface to make electrical contact, the form factor allows the probes to be placed in small physical spaces in close proximity to the areas of interest. For this work, the area of interest is the laboratory created corrosion pit used for crack initiation. The form factor of the DCPD leads are important because of the stress concentrations generated by the pits. Large attachment methods could potentially have larger associated stress concentrations and change the nucleating feature away from the corrosion pit. The engineering challenge from the latter requirement becomes evident when dealing with small crack nucleating defects such as corrosion pits. The stress concentration due to the wire attachment can be greater than that of the corrosion pit causing fatigue nucleation at the lead attachments. Additionally, lead wire placement and spacing have precision and accuracy effects on the measured DCPD signal voltage. A protocol was developed solely devoted to producing a robust lead wire attachment to the specimen through micro-spot welding of copper or platinum wire.

Specimen preparation involved three major areas, specimen pitting, DCPD lead wire attachment, and thin film salt application. Since all fatigue cracks in this work nucleated and propagated from a laboratory created pit, a standardized method using best practices for pit creation was developed. The pitting procedure and DCPD lead wire placement were required for each test specimen, and keeping the preparation between specimens consistent was required for production of repeatable data. For that reason, each of the major preparation steps used best practices to produce consistently prepared specimens. In this testing a laboratory generated corrosion pit is created on the corner of the hole bore where it intersects the planar surface. These laboratory generated pits are formed from an electro-chemical process which produces a rough surface morphology that is similar to pits observed from surveying in-service damage. The rough surface morphology is desired because the typical crack nucleating features tend to be micro-pits that form at the bulk material and pit surface interface [5]. Figure 2 depicts the typical crack nucleating micro pit. Scanning Electron Microscope (SEM) fractography was used to confirm that the laboratory generated pit was the nucleating feature of the fatigue cracks. Full details of the pitting procedure can be found in reference [6]. An overview of the basic steps in the pitting protocol is outlined as follows:

I. Make a hole of the same diameter size as the desired pit in a piece of vinyl tape.
II. Adhere the tape with the hole centered on the desired pit location.
III. Mask off all areas of bare metal aside from the hole in the tape and an area for the constant current lead to be attached.
IV. Submerge the specimen in the pitting solution.
V. Apply a constant current through the specimen.
VI. Allow the electrochemical reaction to take place for the desired amount of time to produce the desired pit size. A table relating current and desired pit size is shown in the full procedure.

Once the specimen has been pitted the next step was the attachment of the DCPD wires to facilitate crack length monitoring. Crack length measurement using the DCPD method requires spot-welding of DCPD measurement probes (copper or platinum wires) to the sample surface. An in-house designed and manufactured welding stage was utilized for repeatable spot-weld location. The electrode used in the spot welding process is machined and polished to reduce its dimension to facilitate smaller weld joints and better placement of the probe wires on the AA7075 specimens. Figure 3 shows the spot welded copper wires (0.127 mm) and platinum wires (0.127 mm) on AA7075 specimens. Consistent probe spacing is required to provide good DCPD resolution. For consistent placement of the DCPD leads a special fixture was used. This spot welding fixture consists of a translation stage with specimen specific holders to locate the open hole specimens under a stereo microscope. This allowed DCPD leads to be positioned with increased accuracy. The DCPD signal resolution is dependent on specimen material, specimen geometry, experimental setup and experimental environment. Early experiments revealed that probe spacing predominantly influences the DCPD voltage signal. The probes placed closer to the corrosion pit increase the signal's sensitivity to crack growth, but the raw DCPD signal value is decreased with corresponding decrease in the signal-to-noise ratio. Probes placed farther apart on either side of the corrosion pit increases the signal-to-noise ratio but the DCPD voltage will be less sensitive to crack growth. Therefore, an optimum distance of 1.0 mm was used as the recommended probe spacing for the open hole specimen throughout fatigue testing. The probe spacing also has the secondary effect of impacting the ability to protect the leads during testing. As the probe spacing decreased the difficultly in properly covering the leads increases because there is a finite amount of space between the hole edge and the lead wire attachment location. Locating the DCPD leads with an offset from the hole edge is required to avoid compounding the stress concentration (K_t) of lead weld with the K_t of the hole, as well as leaving space to protect the leads from environment. Material selection for the DCPD lead wires are typically a choice between copper and platinum. Copper wires were originally used for spot

welding on AA7075 specimens however, as the pit sizes decreased the damage due to the copper spot weld began to approach the stress concentration of the pit and would occasionally nucleate fatigue cracks. Initiation due to welding damage was observed during initial test development. To alleviate the damage due to copper spot welding a switch to platinum lead wires was investigated. This change in material helped to reduce the stress concertation at the spot-welds, however durability issues necessitated a return to copper wire during full immersion and atmospheric tests as the galvanic potential difference between aluminum and platinum made lead protection a priority. The DCPD sensing wires were attached according to the spot welding protocol with the basic steps outlined below and the full method discussed in reference [6].

I. Affix the specimen into the specimen holder under the microscope.
II. Clean the surface of the specimen and the leads (aka DCPD sensing leads, probe wires or probes) of the DCPD wire with alcohol or other degreaser to prepare the sur-face for welding.
III. Temporarily secure the leads of the specimen near the pit.
IV. Position the DCPD leads as near to the pit as possible without damaging the specimen surface near the pit.
V. Lower the spot weld probe tip into contact with the DCPD wire.
VI. Fire the electric pulse.

Testing under atmospherically relevant conditions required a method to deposit thin layers of contaminates onto the specimen surface. For this work sodium chloride was used as the corrosive contaminate based on its efficacy and solubility. To create the thin layer of salt on the specimen surface, this test method refined a hand deposition method for creating the atmospherically relevant thin film on the open hole specimen surface. Methanol was used as the medium in which to transport the salt in order to form an even coating on the specimen surface. This was achieved by dissolving sodium chloride in methanol at a ratio of 140 mg of NaCl per 50 ml of methanol. The mixture was then dispensed by pipet onto the specimen surface at a dosing rate of 400 micrograms per square centimeter. The 400 microgram salt load was chosen to provide an accelerated test with respect to measured atmospheric deposition rates [7]. The next step was to heat the specimen with the heat gun to approximately 54 °C. At this temperature, the surface was hot enough that when a drop of the salt solution hits the specimen the methanol evaporates immediately leaving behind the salt in an even coat where the droplet hit the specimen surface. Droplets were then spread about the surface in multiple raster passes with each subsequent pass offset slightly from the previous pass. The multiple passes of drops produced an evenly coated surface. The surface may require reheating to keep the temperature in this range. Heating the surface much beyond a surface temperature of 60 °C would bring the methanol beyond its Leidenfrost point. At this point the methanol stayed in its droplet form with a thin layer of air insulating the droplet from the specimen surface. This kept the droplet from evaporating at the intended deposition location. Additionally, the air insulation allowed the droplet to move around on the specimen surface frequently causing the droplet to fall off the specimen. The hand deposition method can be summarized by the following:

VII. Mix methanol and salt to the desired concentration
VIII. Heat specimen to approximately 54 °C
IX. Dose specimen with pipet, repeat as necessary to achieve the desired salt loading

Once pitted, welded, and DCPD leads protected with epoxy, all specimens were fatigue tested using a servo-hydraulic load frame. All fatigue testing was performed at a maximum applied stress of 125 MPa with a variable amplitude marker spectrum at a stress ratio (R) of 0.65. The marker spectrum was a sequence of loads applied in blocks to produce visible markers on the fracture surface. The spectrum alternated between load cycles at 100 percent of the maximum applied load and 80 percent of the maximum load in bands of 100 and 10 cycles. This is graphically represented in Figure 4. These visible markers were then used to correlate crack length to cycles during post-test data analysis allowing for reconstruction of the crack path and growth rates. An scanning electron microscope (SEM) image showing typical markers as observed on the post-test fracture surface are seen in Figure 5. Fatigue testing was split into three environmental conditions, laboratory air, full immersion, and atmospherically relevant thin film testing. Baseline fatigue tests were conducted in laboratory-air using DCPD methods to collect fatigue crack growth rate data. Specimen loading was conducted with the variable amplitude “marker band” test spectrum to aid in post-test crack growth reconstruction. Post-test fracture surface reconstruction was carried out via SEM. The post-test reconstruction of the fracture surface provided critical information required to calibrate the open hole test specimen by relating crack length to cycles. All laboratory air tests were conducted at a maximum remote stress (S_{max}) of 125 MPa, maximum applied load (P_{max}) of 4 kN at a stress ratio of R = 0.65 and a frequency of 10 Hz. After the fatigue test concluded, markers on the fracture surface were located in relation to the root of the lab induced corrosion pit. The measured marker locations were coupled with known cycle counts to enable reconstruction of the specimen crack front creating correlation between the crack length and cycle count. Knowing the reconstructed crack growth history allowed the estimation of key points of interest, such as nucleation time and when the periphery crack formation occurred. Periphery crack (a crack that has a continual crack front that intersects both of the plane surfaces) formation is particularly important as this is the earliest time that crack growth predictions can be made. Figure 6 illustrates the mapped data taken from the post-test fracotgraphic measurement of marker bands. Using the normalized DCPD voltage and plotting against the crack lengths measured from the marker bands a calibration curve relating normalized DCPD voltage to crack length can be created. Figure 7 shows the calibration curve for the open hole specimens. Fitting a 6th order polynomial trend line for each of the two crack directions provides equations that relate each of the two crack directions to a single normalized voltage. By separating the two crack directions, both the ‘a’ and ‘c’ direction crack lengths are correlated independently. The results generated in laboratory air can be applied to the open hole specimen to create crack growth calculations for subsequent tests in varying environments. The baseline testing also validated crack growth models in order to calculate the beta correction factors needed to calculate stress intensity values. Once the crack lengths were known, it was then possible to calculate the stress intensity factor (K), and plot the crack growth rate curves for each test. AFGROW was used to calculate the Beta correction factors and resulting stress intensity factor based on the measured marker band crack lengths. These calibrations are required to be done in air, as most of the other environments will corrode the fracture surface and render the marker measurements unresolvable.

To be a successful test method, the developed methodology must be able to detect the changes in crack growth rates due to changes in environmental parameters. To validate the test method two full immersion environments known to accelerate and inhibit crack growth rates were used [8]. The aggressive environment was introduced to prove the test method can generate the required data to detect acceleration in crack growth as well as be durable enough to collect quality data throughout the test. The first full immersion test was

prepared by creating a 150 µm diameter pit at the corner of the hole according to the pitting methods outlined earlier. Once pitted, the DCPD leads were spot welded, using the spot welding protocol, to the specimen and the specimen was secured in the test chamber and filled with 0.06M salt water solution. The specimen was then tested with the 10-4-6 marker spectrum until fracture. The open hole fatigue specimens tested in full immersion were identical in geometry to those tested in the laboratory air calibration work. The loading conditions between the laboratory air and full immersion testing were also kept constant at the 125 MPa stress level. The test frequency was slowed to 1 Hz in immersion whereas the test frequency was 10 Hz in laboratory air. The reduction in test frequency allowed more time for the environment to affect the exposed crack tip for each load cycle. The reduction in test frequency was performed such that the load rate was changed, keeping the crack tip open for a consistent amount of time. The change in load rate was required to keep the time between cycle peak to cycle peak at one second in order to maintain the 1 Hz test frequency regardless of cycle amplitude. The stress ratio of 0.65 also increases the amount of time the crack is open which maximized the effect of environment. If the test frequency is too fast, the environmental effect is minimal producing results closer to those in air. This test frequency also affects the potential efficiency of future testing when added corrosion inhibitor will be added to the environment. In order to keep the frequency consistent between test conditions it was required to be fixed at this time and account for both test conditions. The 1 Hz test frequency is ultimately a trade-off between test duration and time of crack tip exposure to environment. The test cell shown in Figure 8 was constructed from two Polytetrafluoroethylene (PTFE) endcaps clamped to a glass cylinder. O-rings seal both the top and bottom caps to the glass cylinder. The round specimen bottom is also sealed with an O-ring with pressure applied to a sealing plate providing clamp-up to form a seal between the specimen and the test cell. Around the top of the specimen there was a relief where the specimen passed through the upper end cap of the test cell. This relief was provided to ensure that no load could be transferred to the test cell, which would bypass the specimen effectively lowering the applied stress. Tests were conducted until the specimen fractured. This basic procedure was repeated with tests performed in a 0.06M NaCl solution with 0.03M $NaMoO_4$ inhibitor added to the bulk solution. This solution was used to create an environment that would produce crack inhibition. A final series of tests used the same procedure while replacing the full immersion solution with wet air rehydrating a salt film deposited on the specimen surface.

Results

Using the methods and specimen discussed in the Experimental Procedures section, baseline testing was completed in laboratory air at room temperature. The laboratory air testing was performed in order to validate the specimen design by comparing crack growth rate data between the characterized plate of legacy 7075-T651 and data generated using the open hole specimen. This characterized data would serve as a benchmark for all subsequent data generated from the pit-to-crack development work. Baseline testing was performed at a peak stress of 125 MPa and R equal to 0.65. The variable amplitude marker spectrum was used throughout all tests. Fatigue crack growth rates shown in Figure 9 compare the fatigue crack growth rates of the open hole pit-to-crack test specimen and the previously characterized legacy 7075-T651 plate data. Baseline testing showed good agreement between the published legacy 7075-T651 data and the open hole data generated by the open hole specimen. There are some observable differences between the two data sets. One difference appears to be the threshold around ΔK of 3.5MPa$\sqrt{m}$ for the open hole data. This apparent threshold is mostly due to the very small crack growth at the start of the fatigue test coupled with the variable amplitude loading. These two factors make it difficult to discern crack growth from noise at small crack growth. The open hole crack growth data matches the legacy crack growth data very well between ΔK of 3.75MPa$\sqrt{m}$ to 5.5MPa$\sqrt{m}$. After 5.5MPa$\sqrt{m}$ the rate dips below the previous fatigue crack growth rate data. Verification of the dip in crack growth rates was performed by analyzing another set of crack growth rate data from a second geometry. The second geometry was a single edge notch specimen (SEN) fabricated from the same lot of 7075-T651 plate at the T/6 plate thickness. The only difference between the SEN specimen and the open hole specimen is geometry. The SEN crack growth data follows the same trend beyond ΔK of 5.5MPa$\sqrt{m}$. The SEN data dipping below the previously published data suggests well known inter-laboratory variability [9] between the previously generated and current data. Additional noise in the crack growth data was generated by the variable amplitude loading, as the crack growth rate during the 80% marker band cycle still uses the K data from the 100% load cycles. Therefore under the 80% marker cycles an apparent decrease in crack growth is observed. The general trend in crack growth rate still provides a comparison between conditions as the data is consistent across all environments. Future data reduction will address this error by recalculating K for the 80% marker cycles.

The baseline testing showed the specimen and DCPD crack growth calibration worked well for air testing, however the interesting data is produced by the pit-to-crack test methodology when fatigue tests conducted in various environments. While not relevant to operational aircraft, full immersion testing is commonly performed to investigate corrosion fatigue behavior. It is well know that immersion in a chloride solution will accelerate crack growth. The sensitivity required of this test method is such that verification of increased crack growth rates in aggressive environments needed to be confirmed. Verification of test performance was performed with the open hole specimen immersed in a 0.06M NaCl solution. Loading was kept consistent with air data by continued use of the marker spectrum with a 125MPa maximum remote stress and 0.65 R. The test frequency was slowed to 1 Hz for full immersion testing in salt water. Figure 10 shows a comparison of crack growth rates between the open hole specimen in laboratory air and full immersion in saltwater. The result of the full immersion verification tests in 0.06M salt water solution was an upward shift in the fatigue crack growth rate throughout the stress intensity range. The increase in crack growth rate due to the salt solution was the expected result and one that validates the ability of the test method to detect the acceleration of cracking due to an aggressive environment.

With the baseline testing having validated the specimen and DCPD crack growth calibration, and the full immersion testing in salt water providing the expected increase in crack growth rate, the next method that required validation was to show measurable inhibition. A previous study by Warner [10], had already shown that with relatively low concentrations of molybdate, and at low test frequencies (about 1 Hz and below), small amounts of crack growth inhibition were observed. To further validate the test method the open hole specimen was fatigue tested fully immersed in a 0.06M NaCl solution with 0.03M $NaMoO_4$ added. A reservoir of one liter of solution was continually circulated throughout the test duration. Loading was kept consistent with previous testing, using the 125MPa maximum remote stress, with the variable amplitude marker spectrum keeping R equal to 0.65. Figure 11 shows a comparison of fatigue crack growth rates between the open hole specimen in laboratory air, full immersion in salt water, and full immersion in saltwater with added inhibitor. Adding the inhibitor to the salt solution was found to inhibit crack growth at lower ΔK values when compared to the full immersion in salt water specimen. The effect of inhibitor can be seen from a ΔK of approximately 4MPa$\sqrt{m}$ until 5.75MPa$\sqrt{m}$, where the crack growth rate is similar to the specimen tested in air. Beyond ΔK of 5.75MPa$\sqrt{}$

m the crack growth rate increases until it matches the full immersion data. By observing the decrease in crack growth rate between 4MPa$\sqrt{}$m until 8MPa$\sqrt{}$m as compared to the salt water environment, the test method successfully measured crack growth rate inhibition validating the measurement capability.

Open hole specimens tested with thin salt rehydrated by RH were prepared for testing by depositing the salt by the hand deposition method discussed in the Experimental Procedures section. A dosing rate of 400 micrograms of NaCl per square centimeter was used. The front and back of the flat surface of the specimen were covered with salt to maximize the total wetted area. The specimen was then installed inside a modified version of the full immersion test cell in which a dam that surrounds the specimen was affixed to the lower end cap. A mixture of glycerol and water was added to bring the inside of the test cell to a constant relative humidity [11]. The glycerol and water mixture was not allowed to directly make contact with the specimen surface. Figure 12 shows a specimen installed in the test cell and affixed to the test frame. Atmospheric corrosion testing was conducted at 80% relative humidity with a test frequency of 1 Hz. The marker load spectrum with a peak stress of 125MPa was applied with R equal to 0.65 for consistency between all test environments. The specimen was then cycled until fracture. After fracture the specimen was removed from the test cell for fracture surface analysis. Salt was found on the fracture surface confirming that the environment made it into the crack during the test. Figure 13 compares the fatigue crack growth rate curves between the laboratory air, salt water full immersion, and thin salt film specimens. Overall, the hydrated thin salt specimens exhibited an increase in crack growth rate slightly below the full immersion specimens but still accelerated compared to laboratory air data. An interesting aspect of crack rate data is between ΔK of 4 MPa$\sqrt{}$m and ΔK of 6 MPa$\sqrt{}$m. In this region the thin salt film specimen is exhibiting crack growth rates similar to air, however once the ΔK rises above 4.5 MPa$\sqrt{}$m it is approximately the same value as the full immersion specimen. This transition happens very early in the test, where potentially the crack opening is too small to allow the ingress of environment. Once the crack grows larger, the opening displacement is higher and allows the environment into the crack accelerating the crack growth rate.

Discussion

This test procedure was developed to investigate the effect of environment on the nucleation and propagation of fatigue cracks. The goal was to create a test procedure that any reasonably equipped test laboratory could execute by following the stated procedures. Additionally, the test protocol should create test data that can be directly compared from one test site to another. A common test procedure could lead to a greater sharing of data among the research community and aid in the collective understanding of the how nucleation of fatigue cracks from pits can be slowed or stopped. Major components of the test procedure include; methods to create laboratory generated corrosion pits that replicate in-service observed damage, mechanical testing guidance for fatigue testing in both laboratory air and under various environments, and data collection, analysis, and interpretation of the results. The ultimate goal of this test methodology would be widespread acceptance as a standardized method for testing how various environmental factors influence crack nucleation and growth. The test procedures currently have proven to be capable of creating laboratory generated pits of tailored sizes, being able to consistently match fatigue crack growth rates in laboratory air, and capture the reduction of life and influence of environment on test specimens.

An open hole specimen was developed to serve as the standard platform on which the corrosion fatigue test methodology is built. The design of the specimen was envisioned to be easily fabricated with minimal specialty tooling or fixturing required. The specimen hole diameter and gage thickness are common in aircraft construction and the narrow width with respect to hole diameter was chosen to have the stress intensity factor (K) equal at the crack tip along the hole bore and plate surface ideally producing repeatable corner cracks. In addition, this geometry was chosen for its openness to environment, and flexibility for future geometries incorporating filled holes and galvanic couples. The specimens in this program were fabricated from a batch of legacy material. The use of legacy material is an important distinction as modern versions of materials have reduced the amount of impurities in the alloys. The reduction in impurities matter when trying to compare corrosion rates from newly produced materials to those manufactured by original legacy production methods. This is further needed as the original aircraft structure would have been produced using these legacy methods. Particular focus was placed on the iron content of the legacy aluminum, as crack nucleation has been observed from the iron bearing constituent particles [12]. This legacy 7075-T651 material was used throughout the pit-to-crack program because of the characterization work performed during the aforementioned DARPA SIPS program, and the relevance of this material to the sustainment efforts of legacy aircraft.

From test experience the DCPD lead wire material selection becomes a question of durability and protection. Based on the results of the fatigue testing performed during this test program, it can be concluded that copper DCPD leads performed equally to the platinum leads in laboratory conditions and surpass them in atmospheric environments. However a question was raised about the size of the damage site around the spot-welded leads. The weld joints were quantified by performing an investigation during this time. A spot-welded DCPD lead was cross-sectioned and polished to observe microstructural changes caused by the spot-welding procedure. A sample specimen was spot-welded according to the protocol using the standard pointed copper welding tip and an energy level of 7.4%. The spot-welded specimen was sectioned near the aluminum-platinum joint. This sample was then mounted in a Bakelite puck and ground until the fused material was visible in an optical microscope. The surface was then etched such that the aluminum grain boundaries were visible. The typical microstructure around one of the aluminum-platinum spot-welds is shown in Figure 14. In Figure 14, the only area of interest was a small dark area can be seen just below the spot-weld. This area appears to be a small region where the spot-weld energy has possibly affected the base material. The hypothesis was that the discolored area was the dissolution of platinum into the aluminum during the spot-welding process which was then preferentially etched during sample preparation. Of additional note is that grain structure around the weld did not appear to be altered. For the sake of quantifying the damage site, the size of the discolored area was used, even though no microstructural changes were observed as this method would lead to a conservative result. The weld damage site was approximately 50 μm (in the ‘a’ or in the L-S direction) by 20 μm (in the ‘c’ or L-T direction). By comparison a typical pit used during testing was approximately 50 μm in the ‘c’ direction and 40 μm in the ‘a’ direction. These potential damage site sizes were typically smaller than the pit size; however, as desired pit size decreases, the spot-weld damage site may become more critical. It should be noted that during testing all tests nucleated cracks from the corrosion pit rather than the lead wires. The protection of the DCPD lead wires from corrosive attack during fatigue testing is one of the most critical steps in the test procedure. Failure to adequately protect the leads results in a ruined test. To protect the leads, epoxy was applied to the lead wires after spot-welding. A two-layer epoxy coating scheme was used to protect the leads. The first

layer was an epoxy that remained slightly pliable after cure to allow the bonded area a small amount of flexibility. A second epoxy was then applied over the first. The second epoxy was a marine toughened epoxy suitable for salt water bonding. The combination of the two epoxies proved sufficient to protect the DCPD leads of the open hole tests carried out in full immersion. Throughout open hole fatigue testing no specimen properly manufactured and protected nucleated a crack at the copper DCPD lead wire attachment spot welds. The fact that the copper wire spot welded joint did not nucleate any fatigue cracks during testing shows that with proper technique platinum wire is not required. The added reliability from the improved galvanic corrosion resistance between the copper lead wires and aluminum specimen indicates that copper lead wires should be used to insure DCPD lead wire longevity during environmental exposures as long as weld site damage does not occur. The durability gained with copper lead wires is important because as soon as the lead wire attachment fails all subsequent data from the test specimen is lost. The use of multiple spot welded or "stitched" spot welded DCPD leads was found to be lacking as a method for increased durability. The stitched DCPD lead concept, shown in Figure 15, came from a desire to have a secondary sensing path should one of the spot welds fail through a poorly welded connection or through corrosive attack due to a coating failure. In theory, the stitched spot welds appear to provide additional benefits over a single spot weld, but when put into practice the ability of the DCPD leads to sense the small crack growth declined as the multiple spot welds changed the DCPD voltage field. While it would be possible to create a new calibration curve that takes into account the change in DCPD voltage field due to the stitched leads, the use of copper lead wire was a simpler solution. With all things being equal, the discussed lead protection has proven up to the task of adequately protecting the DCPD leads. The time investment to test specimens solely for the new calibration curve would not have been worth the added effort unless long test durations are required and the current protection becomes inadequate.

Methods for hand deposition of thin film salts were developed with the process successfully creating evenly dispersed salt films on the open hole test specimens. After the salt mixture was dispensed by pipet the methanol was then allowed to evaporate, depositing the dissolved salt. Initial trials of salt coverage by the hand deposition method resulted in an uneven coating of salt across the specimen surface. Due to the surface tension in the methanol and changing concentration of salt while the methanol evaporated, the solution would wet the surface and dry unevenly. The deposited salt ring appeared to have increased in concentration at the edges during droplet evaporation. This allowed the salt to produce a thicker layer as the edges dry first and the center last. As the edges dried and the drying progressed inward toward the center, the concentration of salt would build up in the middle of the drop causing a gradient in the salt concentration from the edges to the center of the applied salt solution. The uneven salt concentration produced by the natural evaporation of methanol was insufficient to provide a consistent salt film. It was theorized that an increase in the evaporation rate would help reduce the chances for the salt to form along edges of the droplets. To increase the rate at which the methanol would evaporate forced air was used on the specimen surface while the drops were dispensed from the pipet. A fan was used to force air across the specimen surface while the salt and methanol was applied. This resulted in a quicker drying time, but was not fast enough to prevent the uneven distribution of salt. To produce an even higher evaporation rate a heat gun was used to apply heat directly to the specimen surface. The specimen surface was warmed to approximately 38 °C and the salt and methanol solution was deposited on the surface. The methanol solution evaporated much faster than the forced air method alone, but not fast enough as the salt distribution was still uneven. Additionally during the time it takes for the methanol to evaporate it would rewet previously dried salt and redisperse the salt within the confines of the newly wetted area changing the salt concentration of previously deposited areas. After trying forced air and the lower surface temperatures with little added success, higher specimen surface temperatures were tried. Heating the specimen surface with a heat gun to approximately 54°C proved to be the best solution. In this temperature range the surface temperature was such that the methanol would flash off upon contact with the warm specimen surface. The dissolved salt in the methanol was left behind to form an even area of deposited salt where the droplet had made contact with the specimen surface. This process could be repeated consistently to evenly cover the specimen surface. The even salt surface was required in order to create a equal concentration of salt solution on the specimen surface when exposed to relative humidity. Upon exposure to humid air, the specimen surface would wet out and small water droplets were observed on the two faces of the specimen dosed with salt. The water droplets were spaced evenly across the salt treated surface providing opportunity for the environment to be drawn into the crack and provide acceleration of fatigue crack growth rates. SEM fractography was able to confirm the presence of salt on the fracture surface post-test. The presence of the salt on the fracture surface and the increase in crack growth rate over laboratory air testing proves that the surface deposited salt rehydrated by RH used by the test method is getting sufficient environment into the crack tip to affect fatigue crack growth rates.

Laboratory air testing of open hole calibration specimens provided similar results to the legacy 7075-T651 data. Initial test development was capable of creating a calibration curve relating the DCPD normalized voltage to crack length. This method for crack length calibration is only considered valid for the open hole specimen geometry shown in Figure 1. Any deviation from test specimen geometry, specific DPCD gain settings, or DCPD lead wire spacing could require additional calibrations to maintain data fidelity. It is recommended that fracture surface marker measurements be taken to verify specimen calibration for any change in specimen geometry or DCPD change. The fatigue crack growth data generated from the laboratory air calibration specimen matched the SIPS data very well from approximately a ΔK of 4 MPa$\sqrt{m}$ through ΔK of 11 MPa$\sqrt{m}$. The threshold value observed below ΔK of 4 MPa$\sqrt{m}$ was an artifact of the testing, and should not be considered actual threshold values. To generate threshold values K controlled tests will be required. K controlled tests are possible, but the amount of time to generate threshold data was beyond the scope of this project and do not have as much bearing on the practical crack growth rates observed in the reported data. Above ΔK of 11 MPa$\sqrt{m}$, the crack is approaching the edge of the specimen. As a result, the stress intensity rises too quickly above 11 MPa$\sqrt{m}$ to generate useful data points before the ligament fractures ending the test. Since the crack driving force is so large near the edge of the specimen there is likely little influence of the environment at this point and becomes outside the desired bounds of this test methodology.

Full immersion testing in 0.06M NaCl was successful in that the crack growth rate was found to be accelerated over the entire range of crack growth curve. The fact that acceleration was observed across the entire crack growth curve suggests that the method worked well, as the effect of environment should be more or less constant in full immersion. This effect was observed when looking at the comparison between the crack growth rates collected from the laboratory air specimens, and the specimens testing in the 0.06M NaCl solution. This result is expected as once the crack has nucleated and grown sufficiently large enough to have an open crack tip, the environment was free to act upon the crack tip throughout the remainder of the

test. While the test was ultimately performed to show that the test method could capture the crack acceleration due to environment, the real challenge was the protection of the DCPD lead wires. Initial testing with platinum DCPD wires exposed any weakness in lead protection as the galvanic couple between the aluminum base metal and the platinum DCPD lead was found to be very sensitive to any environmental ingress past the lead wire epoxy protection. To maximize the protection of the spot-welded leads, the location of the spot-weld was moved slightly away from the hole bore. The move allowed more space for the protective epoxy layers to bond to a flat surface more effectively sealing off the environment. A second challenge for lead protection came from the displacement of the specimen. The small amount of stiffness at the ligament meant that a stiff epoxy coating would quickly crack. To alleviate this, two coats of epoxy were used. The first coat was a more flexible epoxy which encapsulated the lead wire itself, while a second layer which was specifically for marine environments was applied over the first coat. The marine toughened epoxy was used to give the coatings additional resistance to the environment effectively protecting the first epoxy layer. The end result was methodology to monitor fatigue crack growth rate in a fully immersed corrosion fatigue environment.

Modern corrosion preventative coatings are designed to not only protect the substrate below the coating simply by covering the material, but by also offering electro-chemical protection as well. The design of these coatings are such that defects in the coating still offer protection from corrosive environments. In some cases the coating chemistry can actually inhibit crack growth [13]. Therefore crack acceleration due to environment is not the only test result of interest. To be truly robust the test method must also measure decreases in crack growth rates in the presence of environments that cause inhibition of the crack growth rate. This is particularly important for research into chromate replacement coatings [14], as equal protection and inhibition of crack growth is desired. Verification of the test method's ability to measure crack growth rate inhibition was conducted by measuring the decrease in crack growth rates of open hole specimens tested in 0.06M NaCl solution with 0.03M NaMoO4 inhibitor added to the bulk solution. This 0.06M NaCl solution was chosen as the base aggressive environment due to both its known amount of crack acceleration, as well as being of lower concentration to the typical 0.6M NaCl concentration. The lower concentration of NaCl was expected to allow the NaMoO4 inhibitor to show an effect, as the goal of this portion of the testing was to show its ability to measure the change in crack growth rate. One liter of the bulk solution was circulated by peristaltic pump throughout the test duration, with no additional aeration of the solution. The test conditions for specimen geometry, applied load, test frequency, test spectrum, and DCPD settings remained identical to the full immersion testing in 0.06M NaCl without added inhibitor. As with the air and salt water immersion testing, specimens were cycled until fracture. Inhibition with respect to full immersion in salt water was proven successful. Full immersion of the open hole test specimens in a 0.06M NaCl + 0.03M $NaMoO_4$ solution resulted in the test data shown in Figure 11. From the fatigue crack growth rates shown in Figure 11 a blanket vertical shift in fatigue crack growth rates due to the environment is not seen. While the vertical shift was observed in the acceleration of full immersion in salt water compared to laboratory air, the inhibited data forms a hybrid dataset between laboratory air crack growth rates and salt water full immersion crack growth rates. The inhibited crack growth rates at lower stress intensity levels exhibit crack growth rates similar to those seen in laboratory air, while at higher stress intensities the crack growth rates became more similar the full immersion in NaCl rates. In between these two regions, is a region showing a gradual transition between the air rates and salt water rates. The transition between the laboratory air to full immersion fatigue crack growth rates can be rationalized based on the protection provided by the inhibitor. At low stress intensities, the crack growth rate is slower allowing the inhibitor time to provide chemical protection, however as the crack accelerates due to the increase in stress intensity, the time the inhibitor has to react with the crack surface decreases providing less protection. The lower amount of protection then begins to allow the environment to begin to accelerate the crack growth until it reaches the portion of the crack growth curve where the mechanical crack driving force dominates. The protection scheme learned from the salt water full immersion testing was also used during the full immersion with good success. Even with the longer duration of inhibited tests lead failure was not an issue. While testing described here was limited to $NaMoO_4$, the method is designed such that any inhibitor is capable of being evaluated.

While full immersion testing provides an easy method to ensure a consistent environment in which to perform a test, it is also desirable to add atmospheric influences into the test method to extend the test method's capabilities to more complex environments. Aircraft are typically exposed to pollutants, airborne salts, and other contaminates while in fight or while stationary in storage on the ground. These contaminates are present on the airframe and can be wetted out by the change in relative humidity (RH) associated with a change in temperature. This change in RH may be due to either ground weather, or the temperature change from ground-air-ground cycles. Once fully wetted out, the contaminants are dissolved into solution and then provide the aggressive environment that can cause or accelerate existing damage. As a result, researchers have an interest in how corrosion fatigue crack growth rates change with these thin films rehydrated by RH. To address this need from the research community, a third test environment was used to investigate the test method's ability to detect changes in crack growth rates due the effects of thin salt films rehydrated by the RH. Like the full immersion tests the same methodology was applied to the open hole test specimens. Use of the salt deposition method applied the salt to the specimen surface, while crack growth was monitored by the same DPCD system as full immersion tests. The final condition that was developed for this test method was the expansion to atmospherically relevant environmental testing. The specimen surface was loaded with a 400 $\mu g/cm^2$ salt concentration, deposited by the hand deposition method developed during this work. Atmospheric fatigue tests were conducted at 80% relative humidity in an effort to create an aggressive atmospheric environment. The 80% RH environment was generated by a mixture of water and glycol. Tests were allowed to soak in environment for one hour prior to the start of testing. This was done to make sure that there was opportunity for the specimen surface to wet and facilitate the salt transportation from the specimen surface to the pit (initially) and the crack tip. The first atmospherically corroded specimens tested at 1 Hz appeared to have longer of a fatigue lives than expected. When looking solely at the number of cycles to failure, fatigue lives came within expected fatigue scatter of the laboratory air tested specimens and it was feared that the environment was not transporting the salt deposited onto the specimen surface into the crack tip. Since the 400 $\mu g/cm^2$ salt loading was developed to be an accelerated test, it was expected that the crack growth would be obviously accelerated. To verify that the salt film was being hydrated and transported into the crack, a fractured specimen was analyzed post-test for evidence of salt ingress. Salt was visible on the fracture surface of the specimen under SEM observation and confirmed with Energy Dispersive X-Ray Spectroscopy (EDS). Visible corrosion was also present on the specimen fracture surface. Since sodium was found on the fracture surface throughout the fatigue crack region it was confirmed that the salt was transported from the specimen surface into the crack. When looking at the fatigue crack growth rates for the atmospheric test a similar trend to that of the inhibitor can be seen. Like the inhibitor test

the crack rates start out similar to air then exhibit a transition to full immersion rates. In the atmospheric tests the fatigue crack growth rate is equal to air from the start of the test until approximately ΔK equal to 4 MPa$\sqrt{m}$. At this point there is an increase of fatigue crack growth rate until it matches the full immersion data at a ΔK of 4.75 MPa$\sqrt{m}$. After ΔK of 4.75 MPa$\sqrt{m}$ the fatigue crack growth rates are approximately equal to full immersion for the rest of the test. What was theorized to be happening at this small crack growth is not the same mechanism as the inhibited tests, as there is no beneficial environment to protect the crack as the specimens are not coated with any type of protection. What is potentially happening is the physical crack size is acting as barrier to the ingress of the salt from the specimen surface. During the development of the lead wire protection it was noticed how the elongation of the specimen ligament was impacting the effectiveness of the epoxy at the leads. In a similar fashion the crack opening displacement will also be dictated by the stiffness of the specimen. So as the crack extends through the ligament, there is a larger change in the crack opening displacement, and with the larger crack opening displacement comes a greater opportunity for the environment to make it into the crack and affect crack growth rates. The similar fatigue crack growth rates of atmospheric and full immersion were also interesting. It was not expected that the crack acceleration would be similar to full immersion crack growth rates. It was expected that the thin film salt would actually be more aggressive than full immersion and show even more crack acceleration. It is thought that the RH levels that helped promote the surface wetting and salt transport into the crack also reduced the concentration of the sodium chloride solution. In wetting and drying scenarios thin salt films have been shown to exhibit higher salt concentrations as they progress through the drying cycle, and lower concentrations as they increase in RH during the wetting phase. In this case relative humidity was held constant at 80% RH. It is possible that even at RH closer to the deliquescence point of sodium chloride, the concentration is still well above the point in which the increase in crack growth rate would be seen making fatigue crack growth rates similar to full immersion plausible. Additionally, it is known that the film thickness influences which mechanism is responsible for the corrosion in the test environment [15], however for this work the film thickness was not measured. This test was designed to show the effects of simulated pollutants rehydrated by the atmospheric conditions and the increase in fatigue crack growth rate. At the higher humidity levels conducted in this test it is possible that film thicknesses were thick enough to mimic the full immersion mechanism resulting in the similar fatigue crack growth rates observed between the atmospheric and full immersion tests. Ultimately the desire is to know what environment effects are begin replicated with this test method, in order to generate results specific to researcher's desired environment. These tests were to show the ability of the test method to capture the potentially subtle changes between environments.

Conclusions

This program successfully developed test methodologies for measuring the effects of environment on the crack growth rates of cracks nucleating from a small corrosion pit. The open hole specimen geometry developed for this test method was validated by creating a crack length calibration curve using the fracture surface data generated during laboratory air testing. The resulting crack growth rates compared favorably to the previously published legacy 7075-T651 fatigue crack growth data. The calibration curves generated from the laboratory air data were then applied to DCPD crack length measurements and crack growth rate data was collected for additional environments relevant to corrosion fatigue research. Open hole specimens tested under full immersion in a salt water solution produced an increase in crack growth rate when compared to laboratory air. The increase in crack growth rate was observed throughout the entire crack growth curve, as expected in a known aggressive test environment. Similarly, when 0.03M sodium molybdate was added to the sodium chloride solution the test method successfully captured the inhibition of crack growth at lower values of ΔK replicating observations made by other researchers. The reduced crack growth resulted in capturing the expected decrease in fatigue crack growth rate. The inhibition effect was pronounced enough that the decrease in crack growth rate increased fatigue life beyond the laboratory air data. Test sensitivity is good enough that trends in initiation data are beginning to form. From the test data it was observed that inhibited crack growth behaved like a hybrid of the air and full immersion data. For small crack sizes at low ΔK crack growth was below the air data (inhibited region), however once the ΔK reaches approximately 6MPa$\sqrt{m}$ the crack growth rate begins increasing until matching the saltwater environment crack growth rate throughout the remainder of the test. Atmospherically relevant thin salt films were successfully applied to the open hole specimen surface through means of hand deposition. The resulting thin salt films were rehydrated with a water and glycerol solution to maintain constant relative humidity inside the test cell. The resulting increase in fatigue crack growth rate was captured by the test method and was found to be similar to full immersion rates when hydrated at 80% relative humidity.

- Successfully developed and refined techniques for using DCPD as a viable crack measurement tool
- Developed techniques for the creation of laboratory generated pits representative of naturally formed pits
- Generated fatigue crack growth rates that demonstrate the method's ability to capture data in multiple environments
- Acceleration in NaCl full immersion
- Inhibition in NaCl +sodium molybdate (Na_2MoO_4)
- Acceleration under thin film conditions
- This work was funded under USAFA Broad Agency Announcements (FA-7000-11-2-0011; FA7000-14-2-0013) by the United States Office of the Secretary of Defense Corrosion Policy and Oversight Office under the Technical Corrosion Collaboration (TCC) and by the Office of Naval Research Science and Technology (N0001413C0113). Research was completed at the United States Air Force Academy Center for Aircraft Structural Life Extension (CAStLE).

References

1. R.P. Wei, et al. (1997), "Corrosion and Corrosion Fatigue of Aluminum Alloys: Chemistry, Micromechanics And Reliability", AFSOR Grant No. F49620-93-1-0426, LEHIGH UNIVERSITY, Bethlehem, PA
2. Z. Gasem, and R.P. Gangloff, "Rate-Limiting Processes in Environmental Fatigue Crack Propagation in 7000-series Aluminum Alloys", in Chemistry and Electrochemistry of Corrosion and Stress Corrosion Cracking, R.H. Jones, Editor. (2001), TMS-AIME: Warrendale, PA. p. 501-521.
3. J.Papazian, E. L. Anagnostou, R.J. Christ, et al. (2009), "DARPA/NCG Structural Integrity Prognosis System", HR0011-04-C-0003. DARPA, Arlington, VA
and Astronautics, 37, 1304-1310
4. J.K. Donald, and J. Ruschau, "Direct Current Potential Difference Fatigue Crack Measurement Techniques" In Fatigue Crack

Measurement: Techniques and Applications, Eds. K. J. Marsh, R. A. Smith, and R. O. Ritchie, Engineering Materials Advisory Service Ltd., Warley, UK, 1991, 11-37.
5. J.B. Burns, R.P. Gangloff, and R.W. Bush, Effect of environment on corrosion induced fatigue crack formation and early propagation in aluminum alloy 7075-T651. DoD Corrosion Conference Proceedings, La Quinta, CA, Aug 2011
6. S.E. Gaylon-Dorman, J.W. Rausch, S.R. Arunachalam, J.T. Burns, R.P. Gangloff, and S.A. Fawaz (2016). Managing Environmental Impacts on Time-Cycle Dependent Structural Integrity of High Performance DoD alloys. SAFE, Inc.
7. I.S. Cole, W.D. Ganther, J.O. Sinclair, D. Lau, D.A. Paterson, A study of the wetting of metal surfaces in order to understand the processes controlling atmospheric corrosion, Journal of the Electrochemical Society, 151, 12 (2004)
8. J.A. Feeney, J.C. McMillan, and R. P. Wei, Metallurgical Transactions, Vol. 1, 1970, pp.1741-1757.
9. P.C. McKeighan, J.H. Feiger, and D.H. McKnight, "Round Robin Test program and Results for Fatigue Crack Growth Measurement in Support of ASTM Standard E647," Final Report, Southwest Research Institute (2008).
10. J. S. Warner, S. Kim, and R.P. Gangloff, "Molybdate inhibition of environmental fatigue crack propagation in Al-Zn-Mg-Cu", International Journal of Fatigue, 2009
11. ASTM D5032-11, Standard Practice for Maintaining Constant Relative Humidity by Means of Aqueous Glycerin Solution, ASTM international, West Conshohocken, PA, 2011, www.astm.org
12. K.M. Gruenberg, B.A. Craig, and B.M. Hillberry (1999). "A probabilistic method for predicting the variability in fatigue behavior of 7075-T6 aluminum", Journal of the American Institute of Aeronautics
13. Lui, X.F., S.J. Huang, and H.C. Gu, Crack Growth Behaviour of High Strength Aluminium Alloy in 3.5% NaCl Solution with Corrosion Inhibiting Pigments. International Journal of Fatigue, 2002. 24(7): p. 803-809.
14. Florent Bocher, James Dante, John R. Scully Samuel Madden and Arwen Wilson, "Scientific Understanding of the Mechanisms of Non-Chromate Corrosion Inhibitors" Final Report SERDP Project WP-1621 (2014).
15. C. Liu, J. Srinivasan, and R. G. Kelly "Electrolyte Film Thickness Effects on the Cathodic Current Availability in a Galvanic Couple", Journal of The Electrochemical Society, 2017 volume 164, issue 13, C845-C855

FIGURE CAPTIONS

FIGURE 1. Typical Open Hole Specimen
FIGURE 2. Scanning Electron Microscopy of micro-pit near the bulk material
FIGURE 3. Typical arrangement of DCPD leads near laboratory created corrosion pits
FIGURE 4. Schematic of applied marker spectrum
FIGURE 5. Scanning Electron Microscopy of marker bands as observed on the fracture surface
FIGURE 6. Example marker measurement and representative fracture surface
FIGURE 7. Calibration curve for normalized DCPD voltage and crack length
FIGURE 8. Open hole specimen installed in the full immersion test cell
FIGURE 9. Crack growth rate comparison between characterized 7075-T651, open hole specimen, SEN specimen.
FIGURE 10. Fatigue crack growth rate data comparing laboratory air and full immersion in salt water
FIGURE 11. Comparison between laboratory air, full immersion in salt water, full immersion in salt water with added molybdate
FIGURE 12. Open hole specimen in atmospheric test cell
FIGURE 13. Comparison of fatigue crack growth rates between laboratory air and hydrated thin salt film test conditions.
FIGURE 14. Schematic showing the standard DCPD spot-weld configuration vs. the stitched spot-weld configuration
FIGURE 15. Micrograph of a cross-sectioned platinum spot-weld

Figures

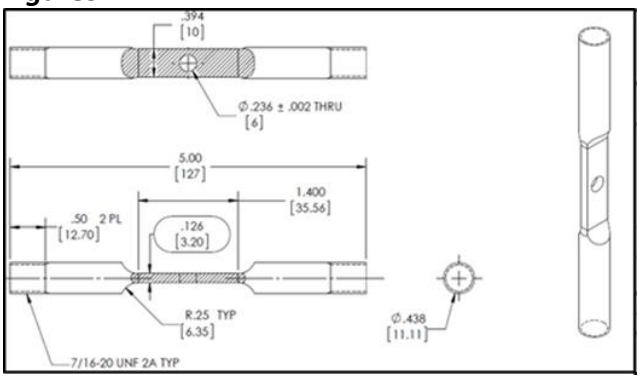

FIGURE 1. Typical Open Hole Specimen, inches [mm]

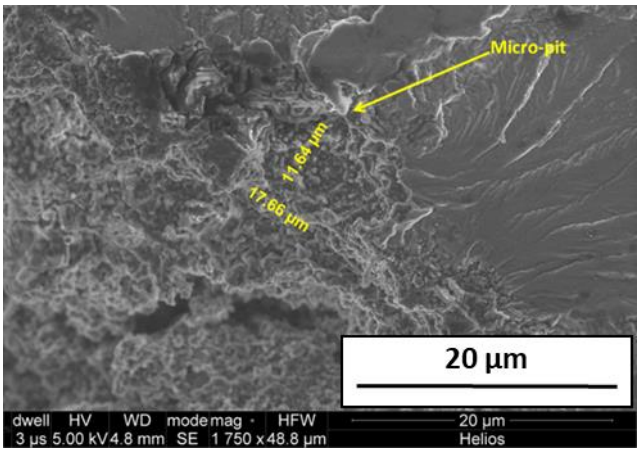

FIGURE 2. Scanning Electron Microscopy of micro-pit near the bulk material

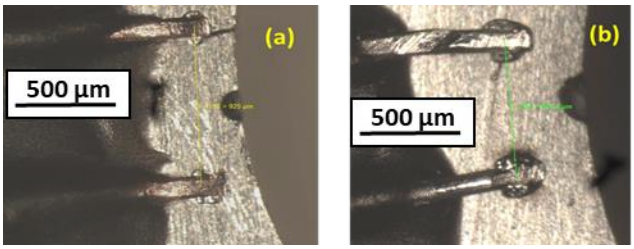

FIGURE 3. Typical arrangement of DCPD leads near laboratory created corrosion pits

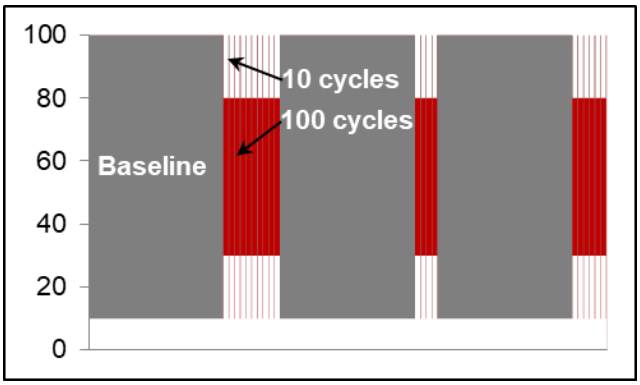

FIGURE 4. Schematic of applied marker spectrum

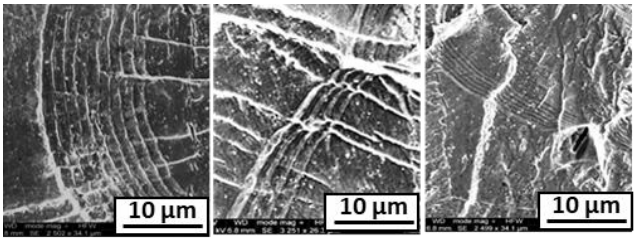

FIGURE 5. Scanning Electron Microscopy of marker bands as observed on the fracture surface

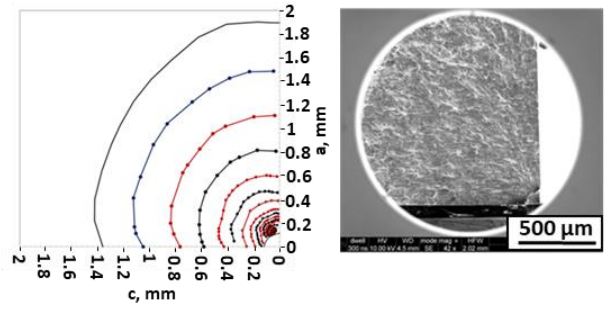

FIGURE 6. Example marker measurement and representative fracture surface

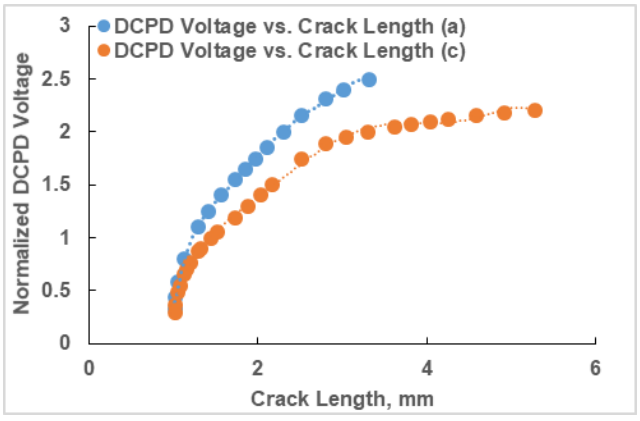

FIGURE 7. Calibration curve for normalized DCPD voltage and crack length

FIGURE 8. Open hole specimen installed in the full immersion test cell

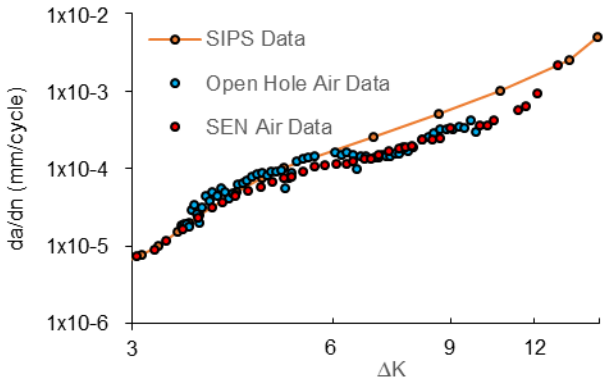

FIGURE 9. Crack growth rate comparison between characterized 7075-T651, open hole specimen, SEN specimen.

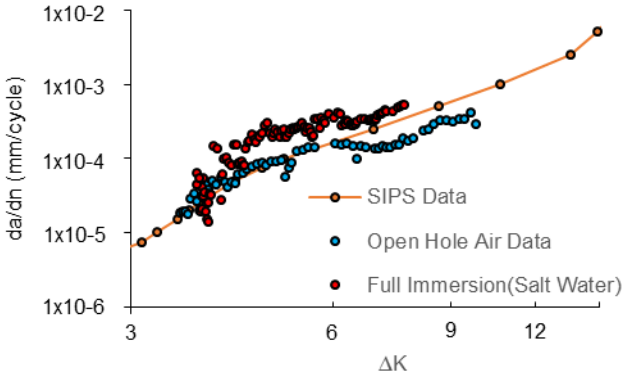

FIGURE 10. Fatigue crack growth rate data comparing laboratory air and full immersion in salt water

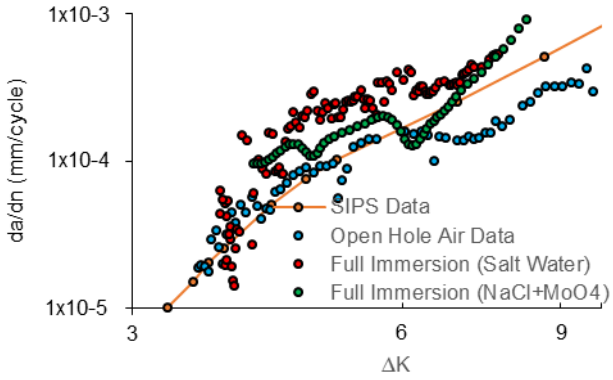

FIGURE 11. Comparison between laboratory air, full immersion in salt water, full immersion in salt water with added molybdate

FIGURE 12. Open hole specimen in atmospheric test cell

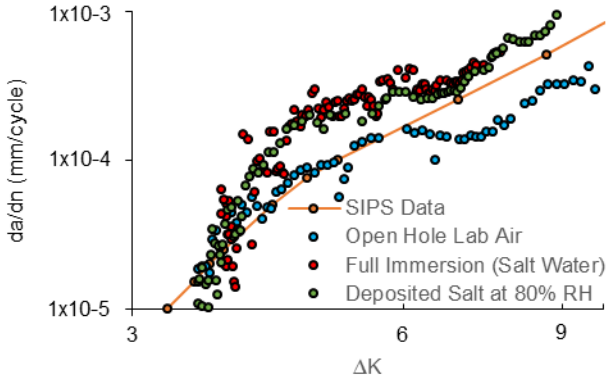

FIGURE 13. Comparison of fatigue crack growth rates between laboratory air and hydrated thin salt film test conditions.

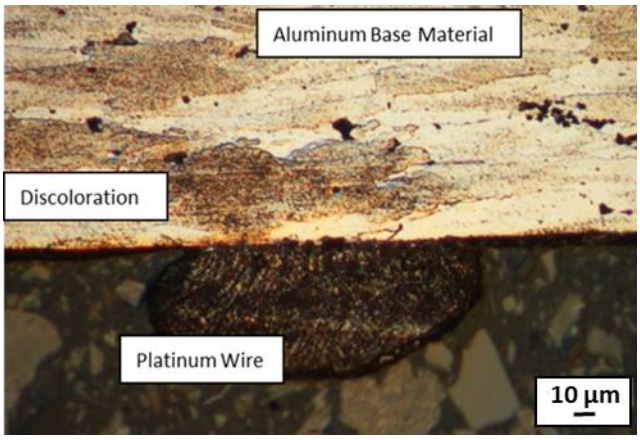

FIGURE 14. Micrograph of a cross-sectioned platinum spot-weld, discolored region indicating potential spot weld damage.

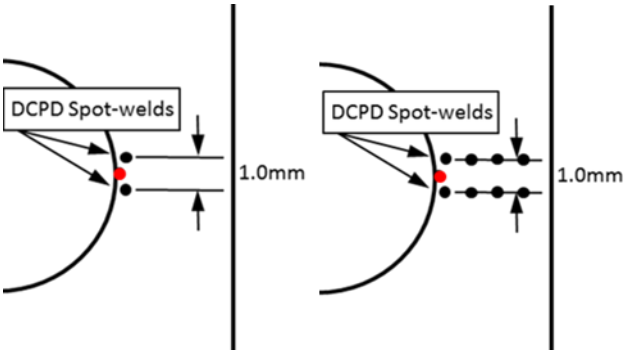

FIGURE 15. Schematic showing the standard DCPD spot-weld configuration vs. the stitched spot-weld configuration